

SCIENTIFIC REPORTS



OPEN

Spatial disease dynamics of free-living pathogens under pathogen predation

Tommi Mononen  & Lasse Ruokolainen

The epidemiological dynamics of potentially free-living pathogens are often studied with respect to a specific pathogen species (e.g., cholera) and most studies concentrate only on host-pathogen interactions. Here we show that metacommunity-level interactions can alter conventional spatial disease dynamics. We introduce a pathogen eating consumer species and investigate a deterministic epidemiological model of two habitat patches, where both patches can be occupied by hosts, pathogens, and consumers of free-living pathogens. An isolated habitat patch shows periodic disease outbreaks in the host population, arising from cyclic consumer-pathogen dynamics. On the other hand, consumer dispersal between the patches generate asymmetric disease prevalence, such that the host population in one patch stays disease-free, while disease outbreaks occur in the other patch. Such asymmetry can also arise with host dispersal, where infected hosts carry pathogens to the other patch. This indirect movement of pathogens causes also a counter-intuitive effect: decreasing morbidity in a focal patch under increasing pathogen immigration. Our results underline that community-level interactions influence disease dynamics and consistent spatial asymmetry can arise also in spatially homogeneous systems.

While epidemiological theory tends to concentrate on obligate pathogens transmitted from host to host (such as measles), many pathogens are actually opportunistically infecting hosts from the environment. Environmental opportunistic pathogens (EOPs) are free-living; they can survive and reproduce in the environment without the presence of a host species (e.g., *Vibrio cholerae* environmental reservoirs found in Haiti¹), but can invade host individuals under favorable conditions. As the long-term survival of the pathogens is independent of hosts, they can cause highly lethal diseases and wipe out even entire host populations^{2,3}. For saprotrophic organisms, killing a host can promote pathogen transmission by an increased growth rate in the dead body⁴. This kind of behavior is highly unlikely for obligate pathogens as the death of an entire host population would also eventually eradicate the pathogens. Examples of EOP diseases include cholera, tetanus, tuberculosis, legionnaires' disease and listeria in humans⁵, anthrax in livestock⁶, Columnaris disease in fish², and white nose syndrome in bats⁷. These diseases are causing deaths as well as economic losses with respect to production animals⁸.

Environmental pathogens living in soil or water encounter predation and competition for resources, which both are decreasing pathogen densities in nature. For example, protozoan predators have been shown to play a significant role in regulating *V. cholerae* in coastal marine waters⁹. These bacterivorous predators include protozoa (ciliates, flagellates and amoebae) as well as more complex organisms (e.g. nematodes)¹⁰. There also exist predatory bacteria, which are using other bacteria as an energy source¹¹. When the density of EOPs is low, they are less likely to infect hosts, while when densities become higher, infections start to emerge in the host population¹². At the same time, predation of the pathogens can increase due to increased consumer densities¹³. However, this predation cannot eradicate the whole pathogen population^{14,15}, which enables also future outbreaks.

Earlier theoretical studies on environmental pathogens have mainly concentrated on local dynamics in a single habitat patch. These studies have demonstrated how outside-host competition can affect disease outbreaks and pathogen invasion ability^{16,17}, and how the predation of pathogens⁸ or their vectors¹⁸ change disease dynamics. Environmental fluctuations have also been shown to play a role in pathogen outbreaks^{19,20}. In general, temporal effects in a single habitat patch are not enough to describe more complex phenomena taking place in nature. An essential part of real-world population dynamics comes from individuals' movements between habitats.

University of Helsinki, Department of Biosciences, Helsinki, FI-00014, Finland. Correspondence and requests for materials should be addressed to T.M. (email: tommi.mononen@helsinki.fi)

Dispersal is an important factor contributing to the spread and persistence of disease epidemics^{21,22}. Obligate pathogens infecting a single isolated host population will run out of susceptible hosts due to acquired host population immunity, or local host extinction. On the other hand, pathogens that can disperse effectively can more easily find the new populations of susceptible hosts. Even if one host population becomes immune, epidemics in other localities, as well as evolutionary changes (or random mutations), can allow for future epidemics in the focal population (e.g. influenza). In real life, diseases spread in spatially heterogeneous environments, and therefore disease dynamics cannot be modeled accurately without using spatial information, influencing spread, emergence, severity²³, frequency²⁴ and persistence²⁵ of an epidemic.

While environmental opportunistic pathogens (EOPs) can survive without hosts, their disease dynamics can also be strongly affected by spatial processes. Existing spatio-temporal studies usually predict the spread of epidemics caused by a single pathogenic agent based on host movement^{26,27}. For example Mari *et al.* noticed that including a human mobility assumption leads to greatly improved prediction of the spread of cholera epidemics²⁸. In this paper, we investigate the spatio-temporal metacommunity dynamics of an environmental opportunistic pathogen in a simple two-patch system, where pathogens are subject to predation in both habitat patches. Each patch contains a population of susceptible and infected hosts, pathogens, and consumers. We consider different scenarios, where either pathogens, consumers or hosts are able to move between patches via random dispersal. Our main hypothesis is that community structure coupled with dispersal will change conventional disease dynamics.

Model and Methodology

Our deterministic continuous-time model consists of two parts: an SIS model for a host-pathogen interaction, coupled with a predator-prey model to describe the interaction between consumers and pathogens. We assume that hosts, pathogens, and consumers occupy two habitat patches, which are connected via dispersal. For host dynamics we assume carrying capacity limited growth, the susceptible-infective-susceptible cycle, and disease mortality. Pathogen dynamics take into account pathogen growth, density-dependent mortality, shedding from infected hosts (hence, pathogen benefits from causing infections), and loss to predation. In consumer dynamics we model, pathogen population size related growth and consumer population decline in the absence of the pathogen. We assume that dispersal rates for susceptible and infected hosts are equal (unless otherwise stated) and we also include dispersal rates for consumers and pathogens.

Epidemiological part. The model consists of two habitat patches denoted by subindices i and j . The epidemiological part (SIS model) is modeled by two equations (per patch):

$$\frac{dS_i}{dt} = r_{\text{host}}(S_i + I_i) - r_{\text{host}}S_i \left(\frac{S_i + I_i}{K_{\text{host}}} \right) - \beta S_i f(P_i) + \delta I_i + d_{\text{host}}(S_j - S_i), \quad (1)$$

$$\frac{dI_i}{dt} = \beta S_i f(P_i) - r_{\text{host}}I_i \left(\frac{S_i + I_i}{K_{\text{host}}} \right) - \nu I_i - \delta I_i + d_{\text{host}}(I_j - I_i), \quad (2)$$

where S_i and I_i are the populations sizes of susceptible and infected hosts in patch i . The pathogen population size P_i is discussed later along with the consumer-pathogen dynamics (see below). Interpretation of all parameters is explained in Table 1. In the susceptible equation, the first two terms are for host growth and carrying capacity related mortality (a logistic growth function). The third term gives pathogen abundance related infection rate and the fourth term gives the rate of host recovery. In the equation for infected, the third term gives a mortality rate for infected hosts. The last term in both differential equations is a host dispersal term, indicating that hosts disperse at a constant rate d_{host} between the patches i and j . The infection rate $\beta S_i f(P_i)$ depends on a sigmoidal infectivity response^{12,16}:

$$f(P_i) = \frac{(P_i/\text{ID}_{50})^\kappa}{1 + (P_i/\text{ID}_{50})^\kappa}, \quad (3)$$

where ID_{50} is a half saturation constant that indicates the dose at which 50% of hosts are infected. The parameter κ defines the steepness of the sigmoidal infectivity response (see Fig. S5a). This response describes natural infectivity phenomenon, where (I) a dose has to be larger than some threshold to cause infections and when (II) the number of infected hosts gets close to full saturation, the growth rate of new infections decreases. Such a response can arise, e.g., when the host immune system can neutralize a small number of invaders, and the infection process (onset of disease) is not instantaneous¹².

Consumer-pathogen part. The consumer-pathogen interaction is modeled with:

$$\frac{dP_i}{dt} = r_{\text{path}}P_i - \mu P_i^2 + \lambda I_i - bg(P_i)C_i + d_{\text{path}}(P_j - P_i), \quad (4)$$

$$\frac{dC_i}{dt} = bg(P_i)C_i - cC_i + d_{\text{con}}(C_j - C_i), \quad (5)$$

where C_i is the size of consumer population in habitat patch i . In the pathogen equation, the first two terms are for pathogen growth and density depended mortality (a logistic growth function). The important third term is λI_i ,

Parameter	Interpretation	Values used in simulations
Epidemiological part		
r_{host}	Host growth rate (per capita)	0.01
K_{host}	Host carrying capacity	100, 200 (default 100)
β	Maximum infectivity	5
δ	Host recovery rate from infection	0.7
ν	Infection kill rate	0.001–0.3 (default 0.01)
d_{host}	Host dispersal rate	0–1.0
Consumer-pathogen part		
r_{path}	Pathogen growth rate (per capita)	1.3
μ	Pathogen mortality (per capita)	0.007
λ	Additional in-host pathogen production (shedding)	0.5
b	Consumer growth rate/consumption rate	0.35
c	Consumer population decline (per capita)	0.36
d_{path}	Pathogen dispersal rate	0–0.1 (default 0.0)
d_{con}	Consumer dispersal rate	0–1.0
Sigmoidal infectivity response		
κ	Slope parameter of the sigmoidal infectivity function	1, 2, 3, 4, 5 (default 3)
ID_{50}	Infectious dose at which 50% of hosts are infected	200
Holling's functional response		
a	Attack rate	0.025–1.125 (default 0.55)
h	Handling time	0.025–1.125 (default 0.45)
q	Shape parameter of the response	1.0–2.0 (default 1.0)

Table 1. A table of model parameters, their explanations and parameter values that are used in the simulations.

which is a continuous shedding of pathogens from infected hosts, indicating that pathogens can reproduce more effectively inside infected host individuals. The fourth term determines a pathogen consumption, where parameter b determines a pathogen consumption rate. In the consumer equation, the second term give the intrinsic decay rate for the consumer population. The last terms describe pathogen and consumer movements between patches. The relationship between predation and pathogen population size is modelled non-linearly using Holling's functional response:

$$g(P_i) = \frac{a(P_i)^q}{1 + h \cdot a(P_i)^q}, \quad (6)$$

where h is handling time of pathogens and a is a constant defining attack rate. When $q = 1$, the response is of type II, and when $q > 1$ the response approaches a sigmoidal type III -function²⁹. Here we assume $q = 1$, if not stated otherwise. The handling time tunes the overall aggressiveness of the consumers; with a short handling time, more pathogens can be eaten per time unit. The attack rate determines effectively how strongly consumers attack a pathogen population at near-zero density (see Fig. S5b). If handling time is short, aggressive consumers make dynamics fast and rough by rapidly consuming the entire pathogen population. On the other hand, ineffective consumers (long handling time) let a pathogen population to survive for a long time. Therefore the handling time affects to conversion efficiency³⁰: with a short handling time, energy moves efficiently, and with a long handling time inefficiently, from the trophic level of pathogens to the trophic level of consumers. With a high attack rate, consumers efficiently reduce the rate of pathogen population growth.

Indirect pathogen flow. To better understand the spatial dynamics in the model, we define two quantities related to population-level movements: (I) an indirect pathogen flow and (II) an effective indirect pathogen flow. Contrary to direct pathogen flow, where pathogens disperse directly from one patch to another, the indirect pathogen flow describes pathogen movement due to dispersing infected hosts. To be precise, it is the amount of pathogen shedding of immigrating infected hosts. Let time points be $T = \{t_1, \dots, t_{k-1}, t_k, t_{k+1}, \dots, t_n\}$, where t_k is a time point with an index k (any continuous-time ODE solver discretizes a time domain). The strength of the *indirect pathogen flow* in the patch j at time t_k is:

$$\text{ipf}(j, t_k) = d_{\text{host}} \lambda_i I_i(t_k), \quad (7)$$

where $I_i(t_k)$ denotes infected hosts at time t_k in patch i . This measure assumes that at the next time step an immigrant becomes a resident and its shedding is no more taken into account. However, if both patches have equal

amount of emigrating infected individuals, the resulting change is zero. Therefore it is better to measure only the net gain:

$$u(i, t_k) = \max [0, \text{ipf}(j, t_k) - \text{ipf}(i, t_k)]. \quad (8)$$

If the number of infected emigrants is larger than the number of infected immigrants, then $u(i, t_k)$ is zero. Now we can compute the *effective indirect pathogen flow* by approximating cumulative net gains during small time intervals that are formed by the sample points T of a ODE solver. By adding all these intervals together we obtain:

$$\mathcal{U}(i, T) = \frac{1}{(t_n - t_1)} \sum_{k=2}^n \left((t_k - t_{k-1}) \frac{u(i, t_k) + u(i, t_{k-1})}{2} \right), \quad (9)$$

where the denominator of a fraction term in front of a sum is the length of a whole observation time interval. This function describes an effective average flow per time unit.

Simulations. The differential equation system is simulated using the Matlab implementation of Dormand-Prince method (ODE45). In all experiments, a long enough transient (at least 2000 time units) is removed to ensure that the system has reached long-term behavior with a given parameter setting. We first visually tracked the lengths of transients using the overly long plots of given dynamics. In addition, we utilized also a doubling procedure, where we doubled the length of a run (and the transient) to ensure that the computed results stay same between two runs. This should confirm that the initial transient was selected to be long enough. The default parameter values were selected to ensure the persistence of the consumer and pathogen in the absence of a host.

Results

Single-patch dynamics and pathogen dispersal. With the default parameters (Table 1), dynamics of an isolated, single-patch system is cyclic. The cyclic dynamics arises from a cyclic consumer-resource interaction, which is in turn mediated to pathogen-host interaction, resulting in infection cycles (Fig. 1a). The infectivity response controls how rapidly an epidemic builds up, and the consumer functional response mainly controls the length and decline of an epidemic.

The direct dispersal of pathogens between patches (e.g., via air, water, or unknown vectors) has a strong synchronizing effect on all populations. Even relatively small pathogen dispersal rates ($d_{\text{path}} \approx 0.01$) are enough to synchronize the patches. This happens because the pathogen directly couples to the consumer as well as the host.

Asymmetric disease prevalence under consumer dispersal. Weak consumer dispersal synchronizes patches, due to its influence on the pathogen populations. However, the situation changes under stronger dispersal (e.g., $d_{\text{con}} > 0.1$). With highly aggressive consumers (handling time $h < 0.1$, coupled with high enough attack rate), the pathogen is unable to infect hosts, as the consumers keep pathogen densities below the infective threshold, imposed by the sigmoidal infectivity response (Fig. 2a). Unexpectedly, less aggressive consumers ($0.1 \leq h \leq 0.27$) generate a persistent asymmetry in disease prevalence, where only one of the patches is disease-free (Fig. 1b).

Synchronized, cyclic dynamics in both patches is achieved with longer consumer handling times ($0.3 < h < 0.9$). Highly inefficient consumers (either high h or low a) are not able to suppress the pathogen, leading to the collapse of the cyclic dynamics. As a result, the system ends up in an equilibrium, where all three species coexist and a considerable proportion of hosts are infected (Fig. 2a).

We will next focus on the properties of asymmetric disease prevalence (Fig. 1b). Firstly, during outbreaks the total number of infected hosts is lower than in the case where both host populations are suffering from the disease. Secondly, the phenomenon is initial value dependent: When the dynamics of the patches are initially in the same phase (equal population sizes in both patches), asymmetry cannot take place. The larger the phase difference, the weaker dispersal is required for asymmetry to emerge. One patch becomes a consumer source that is able to send enough consumers to the other patch (a consumer sink) preventing the rise of epidemic outbreaks in that patch (thorough analysis is in SI, section A). Hence, even if the consumer peaks of the source patch are much higher (Fig. 1b) than the peaks of the sink patch, one determining difference is that the consumers are at the right moment present to prevent the emerging growth of pathogen population. The other difference is that the pathogen population is much smaller than in the source patch, and thereby a small amount of consumers can prevent the pathogen population to grow. On the other hand, there is no pathogen suppression in the source patch as the patch practically follows the single-patch dynamics without any immigrating consumers. Lastly, when carrying capacities of hosts between patches are dissimilar, a host-poor patch can still be a source, if it gets a strong initial advantage and consumer dispersal is strong enough to eradicate pathogen outbreaks in the host-abundant patch.

Sometimes a dynamical behavior that is present in a deterministic system, does not appear in the corresponding stochastic system (e.g. the required precise timing can disappear). Therefore we implemented a stochastic version, and it also shows asymmetry in disease prevalence (see SI, section D). The main difference is that sink and source periods alternate between the two patches due to stochasticity, which is expected as the timing of outbreaks varies and therefore consumers blocking the pathogen growth, may not be present at the right moment.

Disease dynamics caused by indirect pathogen flow. Assuming that infected hosts continue to disperse, their movement creates an indirect flow of pathogens between patches. This reduces the net loss rate of the consumer population and therefore reduces the growth of the pathogen population. This, in turn, acts to dampen the following epidemic outbreak in a patch (see Fig. 1c). When consumer handling time is relatively short (Fig. 2b), outbreak sizes and their intervals vary irregularly—showing chaotic dynamics (Figs 1c and 3), but the system is still interpretable within short time intervals (SI, section B). Stronger shedding (λ) or increased

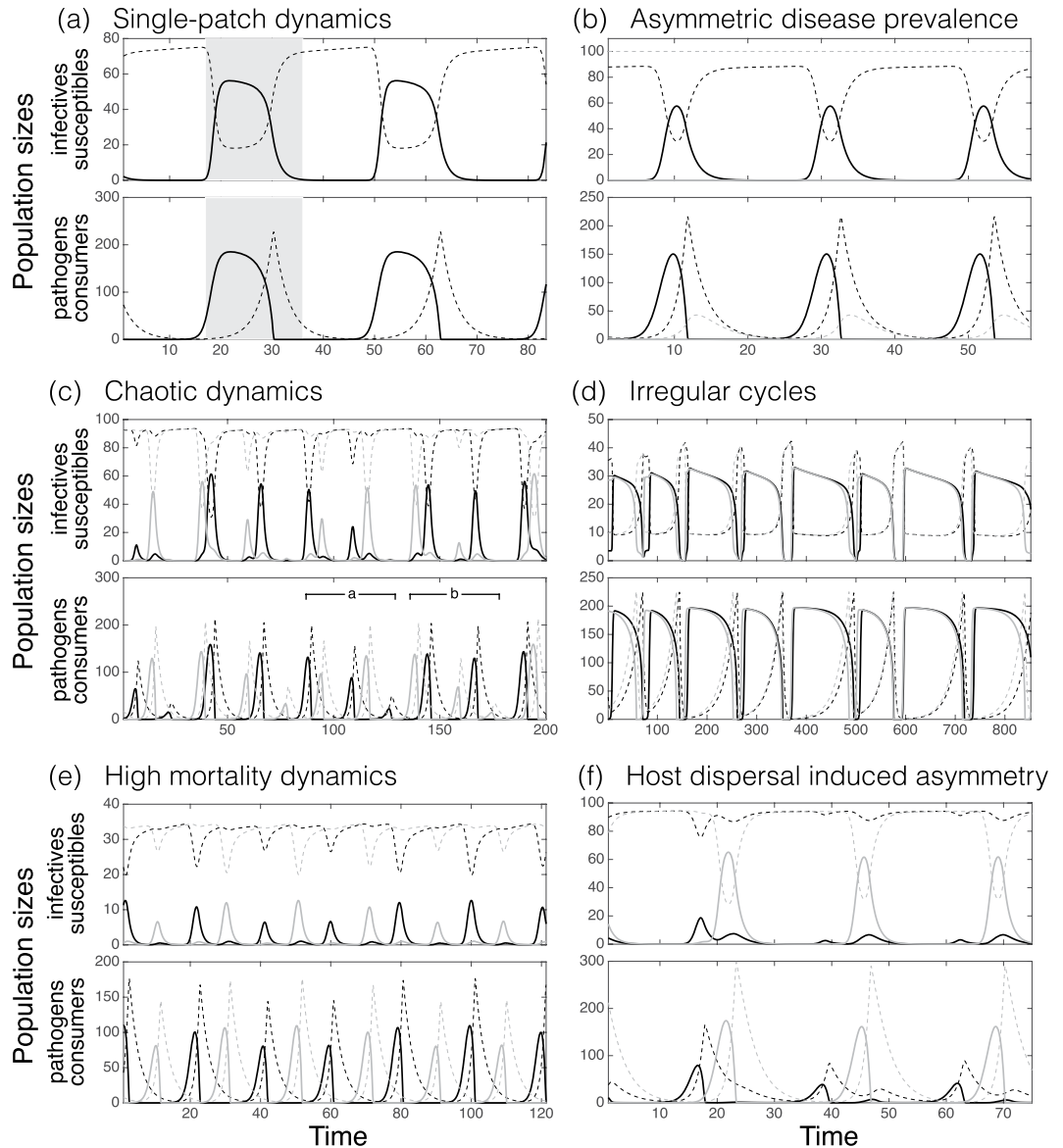


Figure 1. Six different representative classes of cyclic dynamics from model simulations. A line color indicates population's habitat patch (a black or grey patch). In each picture, an upper panel shows the number of infected hosts (solid line) and susceptibles (dotted line) over time and a lower panel shows the number of pathogens (solid line) and consumers (dotted line) over time. **(a)** Single-patch dynamics ($a = 0.55$, $h = 0.45$, $\kappa = 3$, $\lambda = 0.1$), where shaded areas make easier to compare dynamics between infectives and pathogens. **(b)** Asymmetric disease prevalence case (via consumer dispersal) showing one infected and one healthy patch ($a = 0.55$, $h = 0.25$, $\kappa = 3$, $\lambda = 1$, $d_{\text{con}} = 0.15$). **(c)** Example of chaotic dynamics ($a = 0.55$, $h = 0.25$, $\kappa = 3$, $\lambda = 0.1$, $d_{\text{host}} = 0.1$, $\nu = 0.01$), where intervals **a** and **b** show the effect of indirect pathogen flow (sequences of decreasing pathogen populations). **(d)** Example of irregular cycles ($a = 0.55$, $h = 0.85$, $\kappa = 3$, $\lambda = 0.5$, $d_{\text{host}} = 0.1$). **(e)** Example of dynamics under a high mortality rate ($a = 0.55$, $h = 0.25$, $\kappa = 3$, $\lambda = 0.1$, $d_{\text{host}} = 0.1$, $\nu = 0.15$). **(f)** Asymmetric disease prevalence caused by host dispersal ($a = 0.55$, $h = 0.25$, $\kappa = 3$, $\lambda = 1$, $d_{\text{host}} = 0.11$). Notice that population sizes (y-axis) and time intervals (x-axis) vary between panels.

host dispersal rate (d_{host}) acts to increase the indirect pathogen flow. This leads to asymmetric disease prevalence (Figs 1f and 4), due to sustained directional net flow of pathogens from one patch to the other (Fig. 3b). As a result, the consumer population remains at sufficiently high density at all times in one patch.

Increased disease mortality among the hosts weakens the indirect pathogen flow, as infected hosts die more rapidly (Fig. 3e). In addition, if the mortality rate (ν) is sufficiently high, between-patch dynamics become asynchronous (Figs 1e and 3f). In turn, this promotes host metapopulation persistence, as compared to more synchronous dynamics (Fig. 3d, SI, section C). When handling time is long (Fig. 2b), associated with long-lasting disease outbreaks, indirect pathogen flow generates irregularities on the durations of epidemic outbreaks (Fig. 1d). Here the dynamics can be divided into two phases. In an expansion phase, indirect pathogen flow extends the

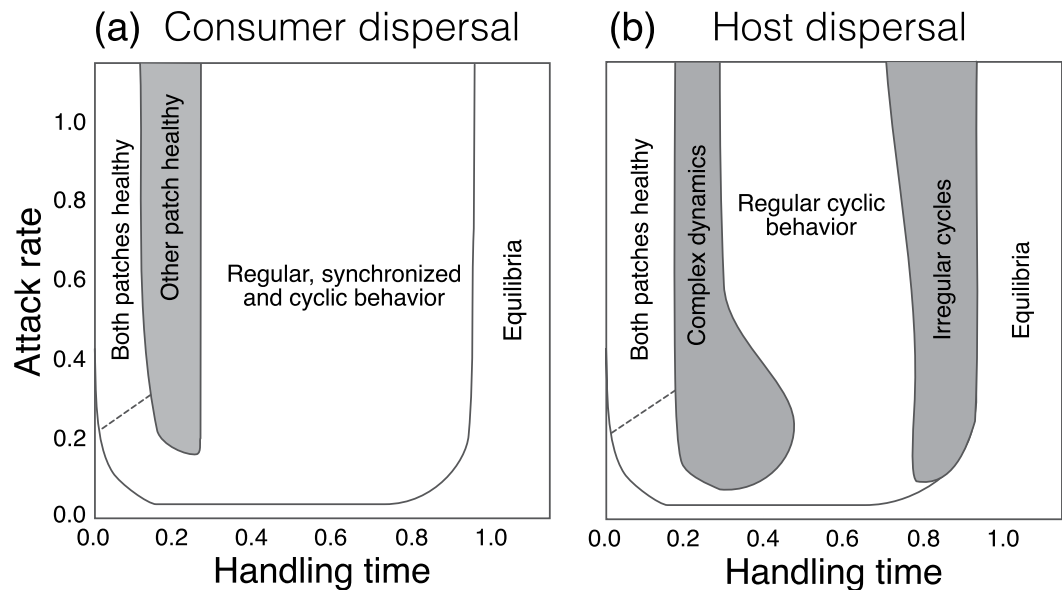


Figure 2. The effect of varying handling time and attack rate on host-pathogen dynamics. In general, cycle lengths increase when a handling time is longer. With a short handling time aggressive consumers make the system disease free, whereas almost all hosts are infected if the handling time is long. **(a)** Areas of different dynamics with the consumer dispersal rate of 0.25 (a large value selected to maximize the effect). **(b)** Areas of various dynamics with respect to the host dispersal rate of 0.1. While parameter values $\kappa = 4$ and $\lambda = 0.5$ were used to produce contrasting patterns, a large range of κ and λ values produces similar dynamical partitions. The dotted line describes a gradual shifting from one dynamics to another and solid borders show an abrupt change in a dynamical behavior. The drawn plots are based on simulation runs with a single representative initial value setting ($S_1 = 90, I_1 = 0, P_1 = 100, Q_1 = 200, S_2 = 10, I_2 = 0, P_2 = 100, Q_2 = 10$). Initial values have influence on shifts between different dynamics and therefore these plots give only approximate dynamical ranges. Hence, near the border area of two different dynamics, the system may end up either of stabilized dynamics depending on the initial balance between different populations.

difference between cycle duration between patches. In a contraction phase both cycles become much shorter than without indirect pathogen flow (Fig. S3; see SI, section B for additional information).

We use the term *complex dynamics* to consist of all dynamics from complex periodic deterministic dynamics to chaotic dynamics. The division between complex dynamics and irregular cycles is made, because indirect pathogen flow acts different way in these two categories (see SI, section B for additional information).

Density-dependent host dispersal: susceptibles avoid infected hosts. The asymmetrical disease prevalence can also be achieved by modifying dispersal assumptions. Here we consider a density-dependent dispersal scenario, where infected hosts are not able to disperse and susceptibles try to avoid them by moving to the other patch (without knowing the situation there). The movement of susceptibles is increased in response to the number of infected hosts I_i in a patch i as $\text{mexp}(\alpha I_i)$ (a related idea in Abrams *et al.*³¹). The parameter m is a basal dispersal rate and α determines the steepness of the exponential curve. When the curve is very steep, susceptibles have a strong avoidance towards infected hosts. This behavior has three consequences: (I) infected and susceptible hosts occupy mostly different patches, (II) epidemics stay small as there are no susceptible hosts present, and (III) the total amount of hosts decreases as one of the two patches is almost abandoned. On the other hand, if we make the basal dispersal rate and the steepness of the exponential function nearly independent of each other and increase the basal dispersal rate, synchronization between the patches increases and the avoidance effect thereby will become weaker. Thus, the resulting dynamics is a combination of basal random movement and avoidance behaviour.

Discussion

We found that in a spatial host-pathogen-consumer system, consumer and host dispersals can lead to an emergent asymmetry in disease prevalence between patches, as well as more complex local population dynamics. While spatial asymmetry due to consumer dispersal is easy to understand (a spill-over of consumers from one patch maintains the other patch disease-free), it is surprising that the same effect can also emerge under host dispersal (Figs 1f and 4). This happens as strong indirect pathogen flow can maintain a consumer population at a sufficiently high density to suppress pathogen population growth in the outside-host environment. Unlike with consumer dispersal, the healthier patch is not completely disease-free, due to immigrating infected hosts and a relatively slow consumer population response to pathogen population growth. Counterintuitively, this leads to a situation where immigrating infected hosts decrease disease prevalence in a focal patch instead of increasing it (complex dynamics turns into asymmetric disease prevalence case in Fig. 4). At the same time, the host

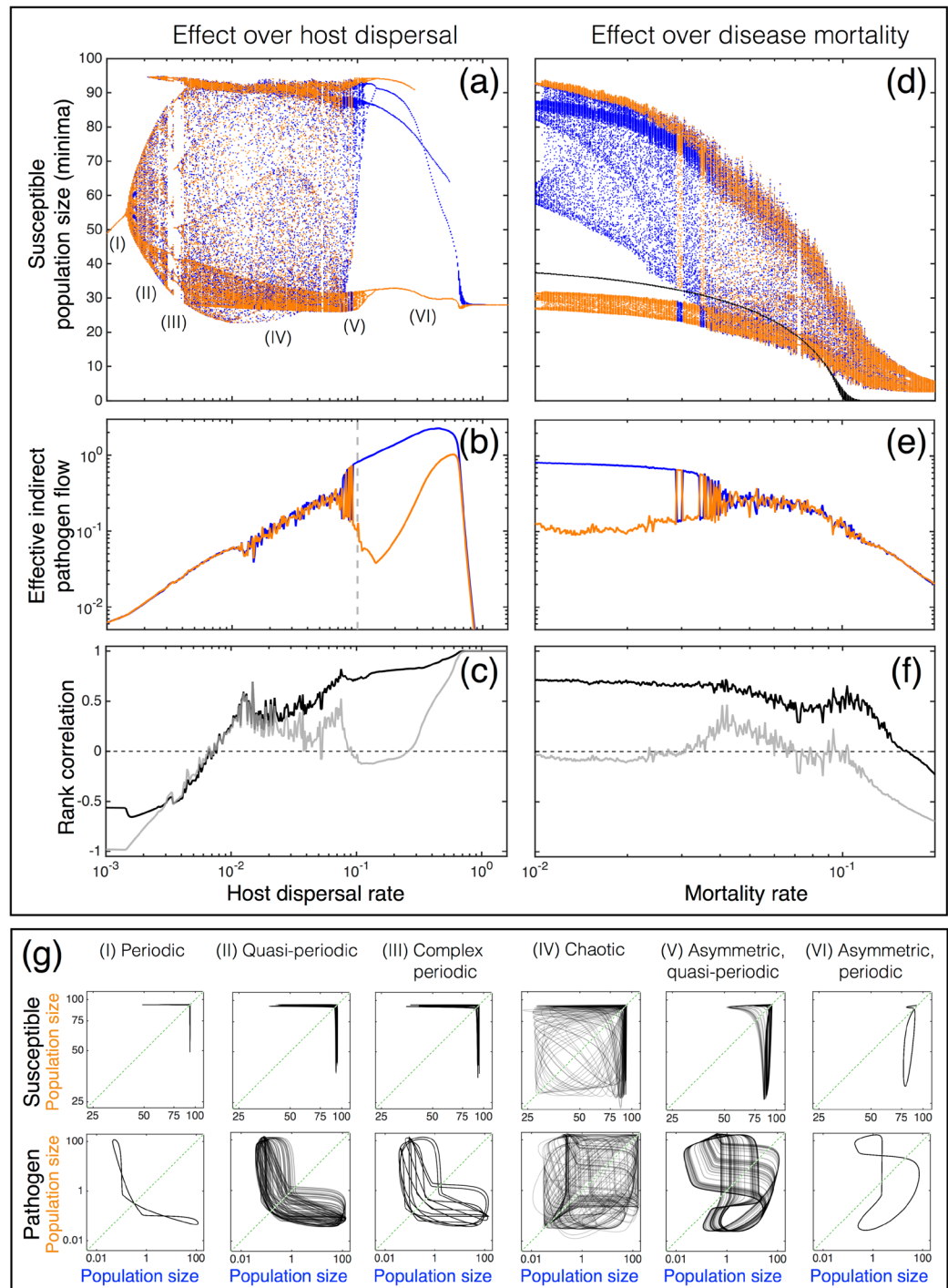


Figure 3. The bifurcation analysis of a chaotic case is presented over host dispersal and mortality rates. **(a,d)** Two bifurcation plots of susceptibles ($\kappa = 3$ and $\lambda = 1$). The colour indicates different patches (blue and orange). In **(d)**, black points represent the bifurcation plot of a double-sized one-patch system (comparable host population size) showing extinction under a lower mortality rate than an asynchronous two-patch system. The next row **(b,e)** represents effective indirect pathogen flow caused by immigrating infected hosts. A dotted vertical grey line on **(b)** shows the host dispersal value (0.1), fixed in **(e)**. Panels **(c,f)** show synchronization between the patches for susceptibles (black line) and for the pathogen populations (grey line). Panels **(a–f)** are computed using the same parameter values and therefore they show different aspects with respect to the same runs. **(g)** Attractors of the susceptible and the pathogen for different dynamical scenarios indicated in panel **(a)**. Label colors match with patch colors. Along increasing host dispersal, the system starts from periodic dynamics (I), moves to quasi-periodic behavior (II) and after that follows chaotic dynamics (IV). As the pressure of indirect pathogen flow further increases the system becomes first asymmetric, quasi-periodic (V) and then asymmetric, periodic (VI). Complex periodic dynamics (III) take place in bifurcation diagrams during phase-locking periods (the behavior of a system becomes occasionally simpler).

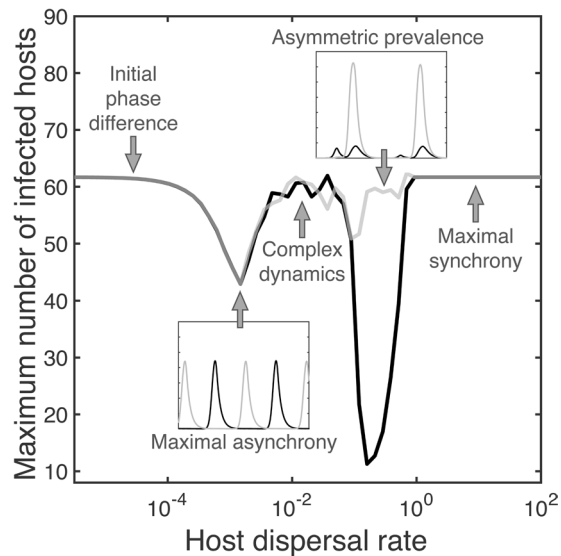


Figure 4. Host dispersal influences the sizes of epidemic outbreaks. Maximum outbreak sizes of two patches are denoted with grey and black curves (averaged over 50 randomly initialized runs, $a = 0.55$, $h = 0.25$, $\kappa = 3$, $\lambda = 1$, $\nu = 0.01$). With very small rates, the two patches are practically independent in their dynamics. The minor movement of infected hosts pushes patches to maximal asynchrony (a lower small panel shows the dynamics of infected host populations) due to better consumer persistence. After the host dispersal range of symmetric complex dynamics, even stronger indirect pathogen flow causes asymmetric prevalence (an upper small panel shows the part of a single run). Finally, the patches become fully synchronised with extremely strong dispersal.

population size stays close to the carrying capacity of the patch, which provides additional evidence that the effect is not caused by somehow increased mortality among infected hosts. These effects persist, even if we add 10% dispersal mortality among consumers or hosts, as long as we compensate the loss of migrants by increasing growth and dispersal rates.

While spatial heterogeneity in population sizes is usually attributed to differences in environmental conditions and/or overall patch quality, which can in turn promote source-sink dynamics or mass effects³², our results indicate that consistent spatial asymmetry can also arise in a fully homogeneous system. In this case, asymmetry is generated by the interplay between interspecific interactions and dispersal. Existing theory on competition assumes that if the competitive environment is homogeneous, coexistence is only possible if there is sufficient intraspecific aggregation in species spatial distributions³³. Such aggregation—which is commonly observed in natural systems³⁴—has not been expected to arise without some ecological differentiation between species³⁵, or heterogeneity in environmental conditions³⁶. Recently, emergent asymmetry in population densities—due to spatial aggregation—in a homogeneous system has been shown to arise under reproductive interference³⁷. It is clear that adaptive behaviour, such as movement, can easily produce out-of-phase dynamics between patches³⁸, as also shown here, or sustained asymmetric spatial distributions in heterogeneous space³⁹. However, our analysis demonstrates that asymmetric disease prevalence, and thus host population size, between identical habitat patches can arise either via a mass effect generated by consumer dispersal, or by indirect pathogen flow due to dispersing infected hosts, associated with increased consumer growth rate in the recipient patch.

Empirical studies are supporting consumer-pathogen dynamics showing density dependence⁴⁰, prey preference (in case of *E. coli* K-12)¹³, and cyclic behavior between protozoa and prey⁴¹, although evolution may affect the latter within some time scale⁴². Pathogen reservoirs can be found from environment¹ and protozoan predators are able to regulate pathogen populations⁹. Host actions⁴³ and dispersal²⁸ spread EOPs and EOP diseases in a landscape. The direct empirical evidence between a strong pathogen flow and decreased infectivity in host populations is missing with respect to our system. However, it has been shown that in highly connected areas (strong pathogen flow), a fungal plant pathogen experiences higher extinction rates than expected due to the higher level of disease resistance⁴⁴. In our system, the strong indirect pathogen flow increases the number of consumers (instead of host resistance), which on its behalf keeps the hosts healthy.

Asymmetric disease prevalence due to consumer dispersal demonstrates a possible biological control mechanism: a small amount of consumers can be introduced at a precise moment to prevent the strong growth of the pathogen population taking place a moment later. Other two options, a constant consumer flow and the introduction of consumers after an outbreak, are less effective. The first one can lead to pathogen immunity against consumers, due to the constant presence of the consumers, and in the latter case, there are already many infected hosts present and a relative large amount of introduced consumers is needed for killing the ongoing epidemics. There have been experiments for using predatory species for biological control^{41, 45, 46} and Merikanto suggested that fisheries could fight against columnaris disease using an artificially created protozoa inflow⁸. Here, we do not model any evolutionary changes in the consumer and pathogen species. However, in reality pathogens are

taking many countermeasures (formed via evolution) to survive from protozoan predation, for example using toxics, surviving in hostile intracellular environment, or by forming biofilm^{47, 48}. The effectiveness of biofilm as protection against predation can, however, be context specific, as some protozoa can successfully feed biofilms⁴⁵. In this study, we also expected a constant virulence throughout time, but in reality pathogen virulence is under evolutionary change as well^{49, 50}.

Pathogen consumers in the outside-host environment can also play an essential role in the stability of local dynamics. In our two-patch metacommunity, both communities contain a food chain of three trophic levels (rather similar to the food chain of hyperparasitism). The bottom level species (host) forms a stable, rich food source for the intermediate consumer, i.e. the pathogen. This might be the reason why we see only stabilizing synchronous effect with pathogen dispersal, although a dispersing intermediate predator species can be destabilizing as well⁵¹. In general, the synchronizing effect of an intermediate level is the strongest as it couples the top and bottom levels⁵². This is also the case in our model, where pathogen dispersal has the strongest synchronizing effect. Here, dispersal at the bottom level is actually hierarchical, as it also causes the movement of the intermediate level species (pathogen), unless host dispersal is restricted to healthy individuals. This sort of hierarchical dispersal can be destabilizing⁵³. Finally, the top level is occupied by pathogen-eating consumers. Consumer dispersal—coupled with practically non-diminishing bottom level resources—collapses the system essentially into a di-trophic food chain, where the pathogen population of one patch may become extinct due to consumer dispersal. Dispersal with respect to different trophic levels can have dissimilar effects on the dynamical behavior of a system, as discussed also in Koelle and Vandermeer⁵⁴.

Any seasonal effects or other stochastic variation, which were not included in the model, can potentially have a huge impact on the dynamics. From one season to the other, growth and mortality rates of different species, as well as dispersal rates, can change in response to changes in environmental conditions. The effects of seasonal and stochastic environmental variation have been studied for example in Anttila *et al.*^{19, 20}, where environmental fluctuations were targeted to have effects on virulence and microbial population sizes. Stronger variation was shown to produce more severe epidemic outbreaks in both cases. In our system, persisting consumer populations can reduce the severity of such outbreaks. The influence of environmental fluctuations on populations in metacommunities can further depend on species dispersal capacity, relative to other members of the community⁵⁵. In addition, how different populations are affected by the environment can also be important^{19, 55, 56}. If we expect distinct environmental fluctuations in each habitat patch, dispersal acts like an averaging force on patch demography. This, however, could mean that an epidemic can spread also to other patch due to host or pathogen dispersal, or dispersing consumers are able to suppress an arising epidemic rapidly. Hence, demographic averaging does not necessarily mean a waning epidemic, but the current state of the system, as well as the dispersal type have a strong impact in each particular case.

While we have assumed a type II saturating functional response for the consumer, the shape of the response is relevant for the presented results. We also tested the sigmoidal response of type III, which is shown to give more stable dynamics than the type II⁵⁷. The areas of complex dynamics and irregular cycles tend to change their dynamic behavior (Fig. S6), shrink, move in the parameter space and even disappear, when tuning the functional response towards the type III. This in turn indicates that the particular shape of the response causes the most observed irregularities. The stabilization happens, because the response of type III is removing the contributions of the smallest pathogen populations. We confirmed this, by shifting the response of type II to ignore the smallest populations and achieved the same effect. A linear functional response (type I) is incompatible with the presented dynamical ranges as it lacks handling time (h) and attack rate (a) parameters. However with the type I, the system shows either equilibrium behavior or regular cyclic dynamics.

Our model bares some similarity with that of Moore *et al.*¹⁸, who analysed the effect of predation on a vector-borne disease. The current model is not directly applicable to vector-borne diseases in general (e.g., due to the assumption of host-independent pathogen growth), but could be easily modified to study the role of dispersal in the dynamics of vector-borne diseases. While this is not within the scope of the present paper, it is an interesting topic for future research.

Our present research reveals that consumer and host dispersal can lead to asymmetric disease prevalence between patches in a homogenous system. Strikingly, morbidity of a focal patch can decrease under increasing host dispersal, although the immigration of infected host becomes stronger at the same time. This happens due to indirect pathogen flow, which arises when pathogens use dispersing hosts as vectors. This flow is also causing complex dynamical effects: outbreak sizes and intervals or their durations become irregular. All these unexpected dynamics will take place only when consumers interact with a host-pathogen system, which emphasizes that (I) a community structure in a free-living stage of the pathogen matters and therefore (II) the constituent species in a community cannot be always safely omitted, as they can have radical effects on disease dynamics¹⁶. Our findings add to the importance of metacommunity interactions in spatial disease epidemics. The link between community ecology and disease dynamics has been recognized as important^{58, 59}, but we stress that species interactions do not occur only between larger, more complex life forms, but also the communities of microbial life forms can have large effects on disease dynamics.

References

1. Alam, M. T., Weppelmann, T. A. & Weber, C. D. *et al.* Monitoring Water Sources for Environmental Reservoirs of Toxigenic *Vibrio cholerae* O1, Haiti. *Emerging Infectious Diseases* **20**(3), 356–363 (2014).
2. Pulkkinen, K. *et al.* Intensive fish farming and the evolution of pathogen virulence: the case of columnaris disease in Finland. *Proceedings of the Royal Society B: Biological Sciences* **277**, 593–600 (2010).
3. Vredenburg, V. T., Knapp, R. A., Tunstall, T. S. & Briggs, C. J. Dynamics of an emerging disease drive large-scale amphibian population extinctions. *PNAS* **107**(21), 9689–9694 (2010).
4. Kunttu, H. M., Valtonen, E. T., Jokinen, E. I. & Suomalainen, L. R. Saprophytism of a fish pathogen as a transmission strategy. *Epidemics* **1**(2), 96–100 (2009).

5. Martínez, J. L. Bacterial pathogens: from natural ecosystems to human hosts. *Environmental Microbiology* **15**(2), 325–333 (2013).
6. Turner, W. C. *et al.* Soil ingestion, nutrition and the seasonality of anthrax in herbivores of Etosha National Park. *Ecosphere* **4**(1), 1–19 (2013).
7. Blehert, D. S. Fungal Disease and the Developing Story of Bat White-nose Syndrome. *PLoS Pathogens* **8**(7), e1002779 (2012).
8. Merikanto, I. Disease dynamics, invasion and biological control of environmentally growing pathogens. PhD thesis, University of Helsinki, Finland (2016).
9. Worden, A. Z. *et al.* Trophic regulation of *Vibrio cholerae* in coastal marine waters. *Environmental Microbiology* **8**, 21–29 (2006).
10. Hoorman, J. J. The Role of Soil Protozoa and Nematodes. The Ohio State University, Fact sheet, Agriculture and Natural Resources (2011).
11. Kadouri, D. E., To, K., Shanks, R. M. Q. & Doi, Y. Predatory Bacteria: A Potential Ally against Multidrug-Resistant Gram-Negative Pathogens. *PLoS One* **8**(5), e63397, doi:10.1371/journal.pone.0063397 (2013).
12. Anttila, J. *et al.* A mechanistic underpinning for sigmoid dose-dependent infection. *Oikos* **126**, 910–916 (2017).
13. Weekers, P. H. H., Bodelier, P. L. E., Wijen, J. P. H. & Vogels, G. D. Effects of Grazing by the Free-Living Soil Amoebae *Acanthamoeba castellanii*, *Acanthamoeba polyphaga*, and *Hartmannella vermiformis* on Various Bacteria. *Applied and Environmental Microbiology* **59**(7), 2317–2319 (1993).
14. Dashiff, A., Junka, R. A., Libera, M. & Kadouri, D. E. Predation of human pathogens by the predatory bacteria *Micavibrio aeruginosavorus* and *Bdellovibrio bacteriovorus*. *Journal of Applied Microbiology* **110**(2), 431–44 (2011).
15. Harini, K., Ajila, V. & Hegde, S. *Bdellovibrio bacteriovorus*: A future antimicrobial agent? *Journal of Indian Society of Periodontology* **17**(6), 823–825 (2013).
16. Anttila, J., Ruokolainen, L., Kaitala, V. & Laakso, J. Loss of Competition in the Outside Host Environment Generates Outbreaks of Environmental Opportunist Pathogens. *PLoS One* **8**(8), e71621, doi:10.1371/journal.pone.0071621 (2013).
17. Merikanto, I., Laakso, J. T. & Kaitala, V. Invasion Ability and Disease Dynamics of Environmentally Growing Opportunistic Pathogens under Outside-Host Competition. *PLoS One* **9**(11), e113436, doi:10.1371/journal.pone.0113436 (2014).
18. Moore, S. M., Borer, E. T. & Hosseini, P. R. Predators indirectly control vector-borne disease: linking predator–prey and host–pathogen models. *Journal of the Royal Society Interface* **7**(42), 161–176 (2010).
19. Anttila, J., Kaitala, V., Laakso, J. & Ruokolainen, L. Environmental Variation Generates Environmental Opportunist Pathogen Outbreaks. *PLoS One* **10**(12), e0145511, doi:10.1371/journal.pone.0145511 (2015).
20. Anttila, J., Laakso, J., Kaitala, V. & Ruokolainen, L. Environmental variation enables invasions of environmental opportunist pathogens. *Oikos* **125**, 1144–1152 (2016).
21. Gurarie, D. & Seto, E. Y. W. Connectivity sustains disease transmission in environments with low potential for endemicity: modelling schistosomiasis with hydrologic and social connectivities. *Journal of the Royal Society Interface* **6**(35), 495–508 (2009).
22. Kyle, J. L. & Harris, E. Global Spread and Persistence of Dengue. *Annual Review of Microbiology* **62**, 71–92 (2008).
23. Thrall, P. H., Godfree, R. & Burdon, J. J. Influence of spatial structure on pathogen colonization and extinction: a test using an experimental metapopulation. *Plant Pathology* **52**, 350–361 (2003).
24. Boerlijst, M. C. & van Ballegoijen, W. M. Spatial Pattern Switching Enables Cyclic Evolution in Spatial Epidemics. *PLoS Comput Biol* **6**(12), e1001030, doi:10.1371/journal.pcbi.1001030 (2010).
25. Hagenaars, T. J., Donnelly, C. A. & Ferguson, N. M. Spatial heterogeneity and the persistence of infectious diseases. *Journal of Theoretical Biology* **229**, 349–359 (2004).
26. Bengtsson, L. *et al.* Using Mobile Phone Data to Predict the Spatial Spread of Cholera. *Scientific Reports* **5**(article 8923), 1–5 (2015).
27. Munch, Z. *et al.* Tuberculosis transmission patterns in a high-incidence area: A spatial analysis. *The International Journal of Tuberculosis and Lung Disease* **7**(3), 271–277 (2003).
28. Mari, L. *et al.* Modelling cholera epidemics: the role of waterways, human mobility and sanitation. *Journal of the Royal Society Interface* **9**, 376–388 (2012).
29. Dawes, J. H. P. & Souza, M. O. A derivation of Holling's type I, II and III functional responses in predator–prey systems. *Journal of Theoretical Biology* **327**, 11–22 (2013).
30. Rip, J. M. K. & McCann, K. S. Cross-ecosystem differences in stability and the principle of energy flux. *Ecology Letters* **14**, 733–740 (2011).
31. Abrams, P. A., Cressman, R. & Krivan, V. The Role of Behavioral Dynamics in Determining the Patch Distributions of Interacting Species. *The American Naturalist* **169**(4), 505–518 (2007).
32. Leibold, M. A. *et al.* The metacommunity concept: a framework for multi-scale community ecology. *Ecology Letters* **7**, 601–613 (2004).
33. Amarasekare, P. Competitive coexistence in spatially structured environments: a synthesis. *Ecology Letters* **6**, 1109–1122 (2003).
34. Gotelli, N. J. & McCabe, D. J. Species Co-Occurrence: A Meta-Analysis of J. M. Diamond's Assembly Rules Model. *Ecology* **83**(8), 2091–2096 (2002).
35. Chesson, P. A need for Niches? *TREE* **6**(1), 26–28 (1991).
36. M'Gonigle, L. K., Mazzucco, R., Otto, S. P. & Dieckmann, U. Sexual selection enables long-term coexistence despite ecological equivalence. *Nature* **484**, 506–509 (2012).
37. Ruokolainen, L. & Hanski, I. Stable coexistence of ecologically identical species: conspecific aggregation via reproductive interference. *Journal of Animal Ecology* **85**(3), 638–647 (2016).
38. Abrams, P. A. & Ruokolainen, L. How does adaptive consumer movement affect population dynamics in consumer-resource metacommunities with homogeneous patches? *Journal of Theoretical Biology* **277**(1), 99–110 (2011).
39. Amarasekare, P. Effect of non-random dispersal strategies on spatial coexistence mechanisms. *Journal of Animal Ecology* **79**(1), 282–293 (2009).
40. Markelova, N. O. The Potential of *Bdellovibrio* For the Biocontrol of the Infectious Agent *Vibrio cholerae*. *Avicenna Journal of Environmental Health Engineering* **2**(2), e4541 (2015).
41. Zhang, J., Örmälä-Odegrip, A.-M., Mappes, J. & Laakso, J. Top-down effects of a lytic bacteriophage and protozoa on bacteria in aqueous and biofilm phases. *Ecology and Evolution* **4**(23), 4444–4453 (2014).
42. Yoshida, T. *et al.* Cryptic Population Dynamics: Rapid Evolution Masks Trophic Interactions. *PLoS Biology* **5**(9), e235 (2007).
43. Chin, C. S. *et al.* The Origin of the Haitian Cholera Outbreak Strain. *The New England Journal of Medicine* **364**(1), 33–42 (2011).
44. Jousimo, J. *et al.* Ecological and evolutionary effects of fragmentation on infectious disease dynamics. *Science* **344**, 1289–1293 (2014).
45. Huws, S. A., McBain, A. J. & Gilbert, P. Protozoan grazing and its impact upon population dynamics in biofilm communities. *Journal of Applied Microbiology* **98**(1), 238–244 (2005).
46. Ravva, S. V., Sarreal, C. Z. & Mandrell, R. E. Altered Protozoan and Bacterial Communities and Survival of *Escherichia coli* O157:H7 in Monensin-Treated Wastewater from a Dairy Lagoon. *PLoS One* **8**(1), e54782, doi:10.1371/journal.pone.0054782 (2013).
47. Barker, J. & Brown, M. R. W. Trojan horses of the microbial world: protozoa and the survival of bacterial pathogens in the environment. *Microbiology* **140**, 1253–1259 (1994).
48. Thomas, V., Herrera-Rimann, K., Blanc, D. S. & Greub, G. Biodiversity of Amoebae and Amoeba-Resisting Bacteria in a Hospital Water Network. *Applied and Environmental Microbiology* **72**(4), 2428–2438 (2006).
49. Massey, R. C., Horsburgh, M. J., Lina, G., Höök, M. & Recker, M. The evolution and maintenance of virulence in *Staphylococcus aureus*: a role for host-to-host transmission? *Nature Reviews Microbiology* **4**, 953–958 (2006).

50. Mikonranta, L., Mappes, J., Laakso, J. & Ketola, T. Within-host evolution decreases virulence in an opportunistic bacterial pathogen. *BMC Evolutionary Biology* **15**(165), 1–8 (2015).
51. Jansen, V. A. A. & Sabelis, M. W. Prey dispersal and predator persistence. *Experimental & Applied Acarology* **14**, 215–231 (1992).
52. Belykh, I., Piccardi, C. & Rinaldi, S. Synchrony in tritrophic food chain metacommunities. *Journal of Biological Dynamics* **3**(5), 497–514 (2009).
53. Pedersen, E. J., Marleau, J. N., Granados, M., Moeller, H. V. & Guichard, F. Nonhierarchical Dispersal Promotes Stability and Resilience in a Tritrophic Metacommunity. *The American Naturalist* **187**(5), E116–E128 (2016).
54. Koelle, K. & John Vandermeer, J. Dispersal-induced desynchronization: from metapopulations to metacommunities. *Ecology Letters* **8**, 167–175 (2005).
55. Ruokolainen, L. Spatio-Temporal Environmental Correlation and Population Variability in Simple Metacommunities. *PLoS One* **8**(8), e72325, doi:10.1371/journal.pone.0072325 (2013).
56. Ruokolainen, L. & McCann, K. Environmental weakening of trophic interactions drives stability in stochastic food webs. *Journal of Theoretical Biology* **339**, 36–46 (2013).
57. Williams, R. J. & Martinez, N. D. Stabilization of chaotic and non-permanent food-web dynamics. *The European Physical Journal B* **38**, 297–303 (2004).
58. Collinge, S. K. & Ray, C. (Eds) *Disease Ecology: Community structure and pathogen dynamics*. Oxford University Press (2006).
59. Johnson, P. T. J., De Roode, J. C. & Fenton, A. Why infectious disease research needs community ecology. *Science* **349**(6252), doi:10.1126/science.1259504 (2015).

Acknowledgements

We thank Peter Abrams, Jani Anttila and Ryosuke Iritani for comments on the manuscript. This research was supported by the Academy of Finland (grant #286405, L.R.).

Author Contributions

T.M. and L.R. designed the model, T.M. analyzed the system partly based on discussions with L.R., T.M. plotted the figures, T.M. and L.R. wrote the manuscript.

Additional Information

Supplementary information accompanies this paper at doi:10.1038/s41598-017-07983-2

Competing Interests: The authors declare that they have no competing interests.

Publisher's note: Springer Nature remains neutral with regard to jurisdictional claims in published maps and institutional affiliations.



Open Access This article is licensed under a Creative Commons Attribution 4.0 International License, which permits use, sharing, adaptation, distribution and reproduction in any medium or format, as long as you give appropriate credit to the original author(s) and the source, provide a link to the Creative Commons license, and indicate if changes were made. The images or other third party material in this article are included in the article's Creative Commons license, unless indicated otherwise in a credit line to the material. If material is not included in the article's Creative Commons license and your intended use is not permitted by statutory regulation or exceeds the permitted use, you will need to obtain permission directly from the copyright holder. To view a copy of this license, visit <http://creativecommons.org/licenses/by/4.0/>.

© The Author(s) 2017